

The Use of Acoustics in Space Exploration

T.G. Leighton

ISVR Technical Report No 314

May 2007



SCIENTIFIC PUBLICATIONS BY THE ISVR

Technical Reports are published to promote timely dissemination of research results by ISVR personnel. This medium permits more detailed presentation than is usually acceptable for scientific journals. Responsibility for both the content and any opinions expressed rests entirely with the author(s).

Technical Memoranda are produced to enable the early or preliminary release of information by ISVR personnel where such release is deemed to be appropriate. Information contained in these memoranda may be incomplete, or form part of a continuing programme; this should be borne in mind when using or quoting from these documents.

Contract Reports are produced to record the results of scientific work carried out for sponsors, under contract. The ISVR treats these reports as confidential to sponsors and does not make them available for general circulation. Individual sponsors may, however, authorize subsequent release of the material.

COPYRIGHT NOTICE

(c) ISVR University of Southampton All rights reserved.

ISVR authorises you to view and download the Materials at this Web site ("Site") only for your personal, non-commercial use. This authorization is not a transfer of title in the Materials and copies of the Materials and is subject to the following restrictions: 1) you must retain, on all copies of the Materials downloaded, all copyright and other proprietary notices contained in the Materials; 2) you may not modify the Materials in any way or reproduce or publicly display, perform, or distribute or otherwise use them for any public or commercial purpose; and 3) you must not transfer the Materials to any other person unless you give them notice of, and they agree to accept, the obligations arising under these terms and conditions of use. You agree to abide by all additional restrictions displayed on the Site as it may be updated from time to time. This Site, including all Materials, is protected by worldwide copyright laws and treaty provisions. You agree to comply with all copyright laws worldwide in your use of this Site and to prevent any unauthorised copying of the Materials.

The Use of Acoustics in Space Exploration

T G Leighton

ISVR Technical Report No. 314

May 2007

UNIVERSITY OF SOUTHAMPTON
INSTITUTE OF SOUND AND VIBRATION RESEARCH
FLUID DYNAMICS AND ACOUSTICS GROUP

The Use of Acoustics in Space Exploration

by

T G Leighton

ISVR Technical Report No. 314

May 2007

Authorized for issue by
Professor R J Astley, Group Chairman

© Institute of Sound & Vibration Research

CONTENTS

CONTENTS	II
<i>ABSTRACT</i>	<i>iii</i>
LIST OF FIGURES	IV
1 INTRODUCTION	1
2 USE OF ACOUSTICS IN EXTRATERRESTRIAL RESEARCH	5
2.1 Construction of artificial acoustic time-series	5
2.2 Interpretation of perturbations in other radiations by appealing to acoustical fluctuations at source	5
2.3 Measurement of acoustic signals introduced by the probe itself	6
2.4 Construction and inversion of the acoustical soundscape.....	6
3 CONCLUSIONS	12
REFERENCES	21

ABSTRACT

In recent years increased attention has been paid to the potential uses of acoustics for extraterrestrial exploration. The extent to which acoustics *per se* is used in these studies varies greatly. First, there are the cases in which acoustics is simply the medium through which some other time-varying non-acoustic signal (such as the output of a cosmic ray detector) is communicated to humans. Second, perturbations in a non-acoustic signal (e.g. EM) are interpreted through mechanisms relating to acoustic perturbations in the source material itself. Third, some probes have made direct measurements of acoustic signals which have been generated by the probe itself, as is done for example to infer the local atmospheric sound speed from the time-of-flight of an acoustic pulses over a short distance ($O(10\text{ cm})$). Fourth, some studies have discussed ways of interpreting the natural acoustic signals generated by the extraterrestrial environment itself. The report discusses these cases and the limitations, implications and opportunities for extraterrestrial exploration using acoustics.

LIST OF FIGURES

Figure	Page
<p>Figure 1. The figure shows several identifiable features on a scale of the frequencies. It is based on a demonstration of such scales, where five markers (indicating, respectively, 20, 40, 60, 80 and 100 kHz) were placed at 1 m intervals from a datum (representing 0 Hz). The figure illustrates this schematically through an unfurled banner, onto a 5m section of which are placed the six markers for 0–100 kHz. The position on this scale of 20 Hz, which is generally taken to be the lowest frequency audible to humans, is shown as being 1 mm from the datum. Above the banner, double-ended arrows indicate important frequency ranges. At the top of the figure, the range of human hearing is shown. The two arrows below that show the ranges typically adopted by several power ultrasound technologies: first, ultrasonic cleaning baths and dental ultrasonics; second, (illustrated by transducers fitted to pipelines and rings of luminescence – Leighton, 2004), power ultrasonic devices for processing materials, for example in pipelines. This frequency range tends to be popular: it is restricted to <20 kHz to avoid hearing hazard, but does not go too high in the ultrasonic range for a number of reasons. These include lower attenuation and the ease at which cavitation can be generated compared to O(100 kHz). Of course, some applications wish to avoid cavitation, and may choose higher frequencies for that reason. The lowest arrow above the banner indicates the fact that this whole range of frequencies is used in the oceans, both by cetaceans and humans. Humans use these ranges for purposes which vary from geophysical surveying at low frequency to zooplankton monitoring at ~100 kHz (Griffiths <i>et al.</i>, 2001) and even using pulses containing energy up to 300 kHz (Holliday, 2001). There are also military uses. Arrows below the banner show that the markers for 1, 5 and 5 0MHz would occur at distances from the datum of 50, 250, and 2500 m, respectively, on this scale. The associated applications (mainly biomedical) are indicated. Six flags are ‘pinned’ into the figure, indicating the wavelength in water λ_w at the frequency where the pin is attached. The wavelength in air λ_a is also shown, but only for the pins at 20 and 60 kHz, artificially to emphasise the fact that, compared to ultrasound in water or metals, applications in air are far more rare at higher frequencies because of the higher absorption there. Taken from Leighton (2007).</p>	2
<p>Figure 2. The figure shows several identifiable features on a scale of the acoustic pressure amplitude. It is based on a demonstration of such scales, where five markers (indicating, respectively, 20, 40, 60, 80 and 100 kPa) were placed at 1 m intervals from a datum (representing 0 Pa). The figure illustrates this schematically through an unfurled banner, onto a 5 m section of which are placed the six markers for 0–100 kPa. Human hearing occupies a small part of this range, as indicated by three flags which have been stacked at the top left of the figure because there is not enough space to pin them in their proper places. At 1.5 nm from the datum is placed the pin indicating an acoustic pressure amplitude of 28.9 mPa, taken to be the threshold for hearing at 1 kHz. At 1 mm is placed the pin for an acoustic pressure of 20 Pa, which would cause pain in humans; and at 1 cm is placed the pin for 200 Pa, which would cause hearing damage in normal human ears. A pair of dividers, topped with a sun, is drawn with its points at 300 Pa and 17 kPa. This is done to illustrate the point that, although even the lower point of the divider (300 Pa) exceeds the threshold for hearing damage, nevertheless the intensities are what physically we might regard as ‘low’. This is because the two point of the dividers correspond to the acoustic pressure amplitudes (in air and water) which would provide in a plane wave the same intensity as daylight. Bright sunshine is considered to be occurring when the solar radiation level exceeds 100 Wm^{-2} (although in actual fact this level would be perceived to correspond to a dull day). Equivalent plane wave intensity occurs in water for zero-peak acoustic pressure amplitudes of 17 kPa in water and 300 Pa in air. The final flag is pinned at the 5 m mark, corresponding to 1 atmosphere of pressure, the threshold for cavitation at low ultrasonic frequencies. Below the scale are arrows indicating tentative values for the acoustic pressure amplitudes which can be measured from a range of biomedical ultrasonic devices operating in degassed water (measurement in vivo in tissue is difficult, but would produce lower values than those that could be generated in degassed water). Additional reasons why these values can only be tentative include the difficulty in assigning pressure amplitudes (to systems shown below the banner) because of the range of waveforms and pulse durations used, the question of whether one refers to the peak positive or peak negative pressure, etc., and because of the acceptable error limits in many ultrasonic measurements. Biomedical applications which are considered to be ‘low intensity’ (physiotherapy, bone health monitoring etc.) occur at respective distances of 10 m and 50 m on this scale (equivalent to acoustic pressure amplitudes of 0.5–1 MPa). Foetal ultrasonic imaging and Doppler biomedical ultrasound are tentatively located at 100 m from the datum on this scale, corresponding to acoustic pressure amplitudes of about 2MPa. The therapeutic applications of HIFU (ultrasonic surgery) and lithotripsy are placed at a range of 5 km on this scale (corresponding to acoustic pressures of 100 MPa). Taken from Leighton (2007).</p>	4

Figure (continued)**Page**

Figure 3. (a) The Salmon Leap, Sadler's Mill, Romsey (Longitude 1°30' W; Latitude 50° 59'N). View to the South-south-west, looking downstream towards the Broadlands estate. The hydrophone was placed at a depth of 10 cm in clear water, about 3 m from the turbulent bubble cloud. (Photograph: T G Leighton). (b) An artist's impression of Titan's surface, undertaken prior to the mission landing. In the sky, Saturn is visible dimly in the background through Titan's thick atmosphere. The Cassini spacecraft flies over the surface with its High Gain Antenna pointed at the Huygens probe as it nears the end of its parachute descent. Thin methane clouds dot the horizon, and a narrow methane spring or "methanefall" flows from the cliff at left and produces considerable vapour. Smooth ice features rise out of the methane/ethane lake, and crater walls can be seen far in the distance. (Illustration by David Seal, Image credit: NASA/JPL/Caltech).

7

Figure 4. In this Cassini radar image, two of Titan's lakes (near 73 degrees north latitude, 46 degrees west longitude) are seen, each 20 to 25 kilometers (12 to 16 miles) across. The image from a flyby on Sept. 23, 2006, covers an area about 60 kilometers (37 miles) wide by 40 kilometers (25 miles) high. They are joined by a relatively narrow channel. The lake on the right has lighter patches within it, indicating that it may be slowly drying out as the northern summer approaches. This image is provided courtesy of NASA/JPL.

8

Figure 5. This side-by-side image shows a Cassini radar image (on the left) of what is the largest body of liquid ever found on Titan's north pole, compared to Lake Superior (on the right). This close-up is part of a larger image and offers strong evidence for seas on Titan. These seas are most likely liquid methane and ethane. This feature on Titan is at least 100,000 square kilometers (39,000 square miles), which is greater in extent than Lake Superior (82,000 square kilometers or 32,000 square miles), which is one of Earth's largest lakes. The feature covers a greater fraction of Titan than the largest terrestrial inland sea, the Black Sea. The Black Sea covers 0.085 percent of the surface of the Earth; this newly observed body on Titan covers at least 0.12 percent of the surface of Titan. Because of its size, scientists are calling it a sea. The image on the right is from the SeaWiFS project, NASA's Goddard Space Flight Center, Greenbelt, Md. (Image Credit: NASA/JPL/GSFC).

9

Figure 6. These two radar images were acquired by the Cassini radar instrument in synthetic aperture mode on July 21, 2006. The top image centred near 80 degrees north, 92 degrees west measures about 420 km by 150 km (260 miles by 93 miles). The lower image centred near 78 degrees north, 18 degrees west measures about 475 km by 150 km (295 miles by 93 miles). Smallest details in this image are about 500 meters (1,640 feet) across. The variety of dark patches in the image suggest the presence of many lakes in the high latitudes around the North Pole of Titan. Some of these dark patches have channels leading in or out of them. The channels have a shape that strongly implies they were carved by liquid. Some of the dark patches and connecting channels are completely black, that is, they reflect back essentially no radar signal, and hence must be extremely smooth. In some cases rims can be seen around the dark patches, suggesting deposits that might form as liquid evaporates. Because such lakes may wax and wane over time, and winds may alter the roughness of their surfaces, repeat coverage of these areas should test whether these are indeed bodies of liquid. (Image Credit: NASA/JPL).

10

Figure 7. Images of Titan obtained by the Huygens probe. (a) This mosaic of three frames provides detail of a high ridge area including the flow down into a major river channel from different sources. (b) A single image from the Huygens DISR instrument of a dark plain area on Titan, seen during descent to the landing site. There appears to be flow around bright 'islands'. The areas below and above the bright islands may be at different elevations. (c) The landing site of Huygens is circled. (Credits: ESA/NASA/JPL/University of Arizona).

10

Figure 8. (a) Cracks on Europa's ice surface. Most scientists believe that salts and other inorganic materials are responsible for the coloured patches on Europa's outer layer, although there has been speculation that bacteria, extruded through the ice from below and 'flash frozen' on the surface, are responsible. (Credit: NASA/JPL) (b) Top left: schematic of possible acoustic-based mission to Europa, where acoustic signals originating from various planetary sources are passively detected and transmitted to Earth via an orbiter (schematic: TG Leighton). Lower: the surface of Europa, showing ice features (Credit: NASA/JPL). Right: Schematic of the interior of Europa, showing ice covering over a water ocean, overlaying the solid interior (Copyright Calvin J Hamilton).

11

Figure 9. The acoustic pressure antinodes within cylinders filled with aqueous solution (with vertical axis of symmetry, and the sound source at the cylinder base) are made visible through the chemiluminescence which occurs there. (a) Plan and (b) side views of luminescence (which occurs at pressure antinodes) in a liquid-filled cell which had a polymethylmethacrylate wall (9.4 cm internal diameter, 10 cm external diameter; height of aqueous solution=14 cm) for insonification at 132.44 kHz where the spatial peak acoustic pressure in the liquid was 75 kPa (all quoted zero-to-peak). Frames (c)-(f) (to which the scale bar of length 5.8 cm in frame (c) refers) were taken in a double-walled, water-jacketed cell (5.8 cm internal diameter, 8.5 cm external diameter, and liquid height 8 cm) which was maintained at a constant liquid temperature of 25°C. For a constant applied drive voltage, as the insonifying frequency changed, so too did the spatial peak acoustic pressure, providing the following combinations: (c) 121 kHz; 139 kPa; (d) 122 kHz; 150 kPa; (e) 123 kHz; 180 kPa; (f) 124 kHz; 200 kPa.. The effect of tuning into particular acoustic modes is evident: a 1 kHz change in frequency can dramatically alter the amount and distribution of the luminescence (Birkin *et al.*, 2003(a,b)). Hence the not uncommon practice of incrementing frequencies by O(100 kHz) when testing for the 'optimal processing frequency' in such arrangements is nonsensical. Similarly, if calorimetry were used to estimate the ultrasonic field, the change of sound speed resulting from the rise in liquid temperature could detune the mode. By noting the modal resonance frequencies in these and similar cylinders, the sound speed in this bubbly water was found to be in the range 868-1063 m/s, implying void fractions of $2.9-4.2 \times 10^{-3}$ %. Frames selected from several figures in Birkin *et al.* (2003(a)). (Figure including data from P.R. Birkin, J.F. Power, T.G. Leighton and A.M.L. Vincotte; taken from Leighton, 2007).

14

Figure 10. Images taken on Oct. 11, 2005 using the Cassini spacecraft wide-angle camera at a distance of approximately 39,000 kilometers (24,200 miles) from Dione and at a Sun-Dione-spacecraft angle of 22 degrees. The image scale is about 2 kilometers (1 mile) per pixel. The camera employed blue, green and infrared (centred at 752 nanometers) spectral filters, which were used to create this colour view, which approximates the scene as it would appear to the human eye. Speeding toward pale, icy Dione, Cassini's view is enriched by the tranquil gold and blue hues of Saturn in the distance. The horizontal stripes near the bottom of the image are Saturn's rings. The spacecraft was nearly in the plane of the rings when the images were taken, thinning them by perspective and masking their awesome scale. The thin, curving shadows of the C ring and part of the B ring adorn the northern latitudes visible here, a reminder of the rings' grandeur. It is notable that Dione, like most of the other icy Saturnian satellites, looks no different in natural color than in monochrome images. (Image Credit: NASA/JPL/Space Science Institute).

17

Figure 11. This ultraviolet image taken from the Hubble Space Telescope shows Jupiter's atmosphere after many impacts by fragments of comet Shoemaker-Levy 9. A large, dark patch from the impact of fragment H is visible rising on the left side. Proceeding to the right, other dark spots were caused by impacts of fragments Q1, R, D and G, and L, with L covering the largest area of any seen thus far. The spots are very dark in the ultraviolet because a large quantity of dust is being deposited high in Jupiter's stratosphere, and that dust absorbs sunlight. Scientists will be able to track winds in the stratosphere by watching the evolution of these features. Jupiter's moon, Io, is the dark spot just above the center of the planet. (Image Credit: Credit: Hubble Space Telescope Comet Team).

18

Figure (continued)**Page**

Figure 12. Extreme Ultraviolet Imaging Telescope (EIT) image of a huge, handle-shaped prominence taken on Sept. 14, 1999 taken in the 304 angstrom wavelength. Prominences are huge clouds of relatively cool dense plasma suspended in the Sun's hot, thin corona. At times, they can erupt, escaping the Sun's atmosphere. Emission in this spectral line shows the upper chromosphere at a temperature of about 60,000 degrees K. Every feature in the image traces magnetic field structure. The hottest areas appear almost white, while the darker red areas indicate cooler temperatures. (Image Credit: Courtesy of SOHO/Extreme Ultraviolet Imaging Telescope (EIT) consortium). **19**

Figure 13. One of the more spectacular changes recorded for Halley during an apparition was the detachment event that happened April 12, 1986. This 3-minute exposure was taken using the Michigan Schmidt telescope at Cerro Tololo Interamerican Observatory. The resulting image clearly shows part of the ion tail structure detached from the comet. At this period, the orientation of the comet is such that the tail is foreshortened, with the prolonged radius vector pointing west of north. (Image credit: NASA/JPL). **20**

Figure 14. Gullies in Sirenum Terra, Mars (Date: 10.03.2006). This enhanced-color view shows gullies in an unnamed crater in the Terra Sirenum region of Mars. It is a sub-image from a larger view imaged by the High Resolution Imaging Science Experiment (HiRISE) camera on NASA's Mars Reconnaissance Orbiter on Oct. 3, 2006. This scene is about 254 meters (about 830 feet) wide. The upper and left regions of this scene are in shadow, yet colour variations are still apparent. The high signal to noise ratio of the HiRISE camera allows for colours to be distinguished in shadows. This allows dark features to be identified as true albedo features versus topographical features. (Image credit: NASA/JPL/Univ. of Arizona) **21**

Figure 15. When NASA's Deep Impact probe collided with Tempel 1, a bright, small flash was created, which rapidly expanded above the surface of the comet. This flash lasted for more than a second. After the initial flash, there was a pause before a bright plume quickly extended above the comet surface. The debris from the impact eventually cast a long shadow across the surface, indicating a narrow plume of ejected material, rather than a wide cone. The Deep Impact probe appears to have struck deep, before gases were heated and explosively released. The impact crater was observed to grow in size over time. A preliminary interpretation of these data indicate that the upper surface of the comet may be fluffy, or highly porous. The observed sequence of impact events is similar to laboratory experiments using highly porous targets, especially those that are rich in volatile substances. The duration of the hot, luminous gas phase, as well as the continued growth of the crater over time, all point to a model consistent with a large crater. This image was taken by Deep Impact's medium-resolution camera. (Image credit: NASA/JPL-Caltech/UMD). **22**

1 Introduction

For much of the history of extraterrestrial exploration, the importance of acoustics has perhaps been underrated. This could stem from several sources. One is perhaps the lack of atmosphere in our most explored extraterrestrial body (the Moon), or in the space in between. Another perhaps stems from the not uncommon perception amongst some non-acousticians that acoustics is a ‘solved’ field, the important equations of which were published a century ago. However the history of a range of applications, from sonochemistry to biomedical ultrasonics, has shown that it can be misleading for scientists and engineers from other disciplines to try to incorporate an acoustical element into their studies by purchasing an inexpensive electret microphone, or by treating acoustic propagation as a simplified version of electromagnetic propagation, without recognition of the need for specialist expertise.

If present, such attitudes perhaps stem from our familiarity with acoustic propagation through the atmosphere at audio frequencies, even though this only comprises a tiny fraction of the current use we make of acoustics (Leighton *et al.*, 2005(a)). This familiarity arises because, of course, acoustics affects our lives profoundly and commonly, both as a nuisance and a necessity, and in a way all of us with normal hearing are ‘experts’. Through speech, acoustics has dominated our communications for millennia. It underpins not only recorded music but also live transmissions, from entertainment in theatres and concert venues to public address systems. Although our experience for millenia has been dominated by audiofrequency sound in air, today we use ultrasound in liquids for biomedical diagnosis and therapy, for sonochemistry and ultrasonic cleaning, and for the monitoring and preparation of foodstuffs, pharmaceuticals and other domestic products (Leighton, 2004, 2007). From the Second World War to the present conflicts, acoustics has had an unrivalled role in the underwater environment (Leighton and Heald, 2005). Underwater sound sources are used to map petrochemical reserves and archaeological sites, as well as to monitor a huge variety of important commercial and environmental features, from fish stocks to climate change. The fall of the Berlin Wall in some ways stimulated greater use of our expertise in underwater and geophysical acoustics to explore the environment, in the developing field of ‘Acoustical Oceanography’ (Leighton *et al.*, 2001; Medwin, 2005).

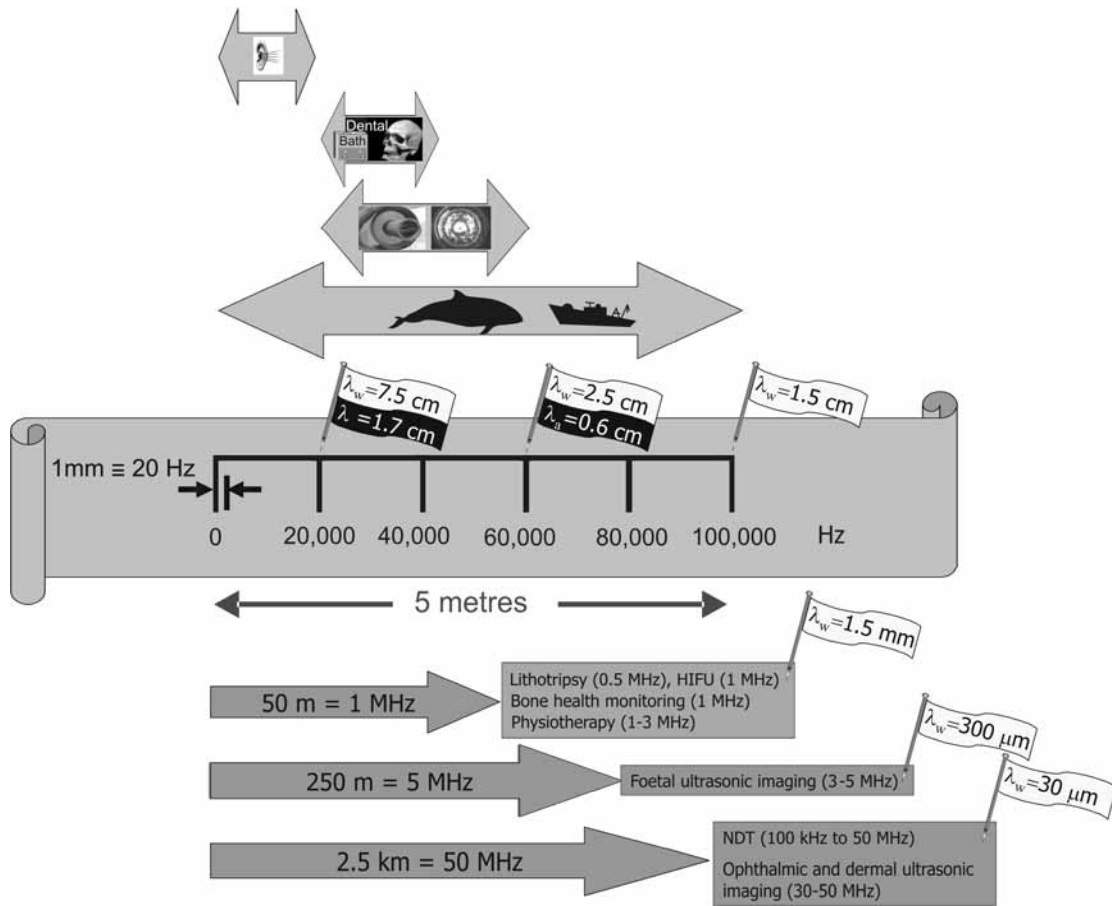


Figure 1. The figure shows several identifiable features on a scale of the frequencies. It is based on a demonstration of such scales, where five markers (indicating, respectively, 20, 40, 60, 80 and 100 kHz) were placed at 1 m intervals from a datum (representing 0 Hz). The figure illustrates this schematically through an unfurled banner, onto a 5m section of which are placed the six markers for 0–100 kHz. The position on this scale of 20 Hz, which is generally taken to be the lowest frequency audible to humans, is shown as being 1 mm from the datum. Above the banner, double-ended arrows indicate important frequency ranges. At the top of the figure, the range of human hearing is shown. The two arrows below that show the ranges typically adopted by several power ultrasound technologies: first, ultrasonic cleaning baths and dental ultrasonics; second, (illustrated by transducers fitted to pipelines and rings of luminescence – Leighton, 2004), power ultrasonic devices for processing materials, for example in pipelines. This frequency range tends to be popular: it is restricted to <20 kHz to avoid hearing hazard, but does not go too high in the ultrasonic range for a number of reasons. These include lower attenuation and the ease at which cavitation can be generated compared to O(100 kHz). Of course, some applications wish to avoid cavitation, and may choose higher frequencies for that reason. The lowest arrow above the banner indicates the fact that this whole range of frequencies is used in the oceans, both by cetaceans and humans. Humans use these ranges for purposes which vary from geophysical surveying at low frequency to zooplankton monitoring at ~100 kHz (Griffiths *et al.*, 2001) and even using pulses containing energy up to 300 kHz (Holliday, 2001). There are also military uses. Arrows below the banner show that the markers for 1, 5 and 50 MHz would occur at distances from the datum of 50, 250, and 2500 m, respectively, on this scale. The associated applications (mainly biomedical) are indicated. Six flags are ‘pinned’ into the figure, indicating the wavelength in water λ_w at the frequency where the pin is attached. The wavelength in air λ_a is also shown, but only for the pins at 20 and 60 kHz, artificially to emphasise the fact that, compared to ultrasound in water or metals, applications in air are far more rare at higher frequencies because of the higher absorption there. Taken from Leighton (2007).

The opportunities to exploit acoustical signals, which can propagate in the oceans and seabed to distances and depths not achievable by EM signals or probes, have been explored extensively over the last decade, with the growth of the use of ‘acoustic inversion’ to estimate key environmental parameters. In acoustical inversion, the measured properties of an acoustical signal (sound speed,

attenuations, dispersion, scatter etc.) are used to estimate such factors as ocean temperatures, bubble populations, zooplankton populations, sediment parameters etc.

In anything but the simplest form of acoustic inversion (such as attributing a signal as caused by lightning rather than self-noise in a detector), a ‘forward model’ is required, which predicts the acoustic parameters from known environmental input. The inversion is usually a more complicated process, where this model is (in common terminology) ‘run backwards’ to try to estimate the environmental parameters from the acoustical data. This might be done through a matrix inversion (Leighton *et al.*, 2004). Given this increase in expertise in acoustics, it would be remiss not to design acoustical measurements in extraterrestrial probes such that the data could be exploited to the fullest capacity (given that such processing will probably occur some years after the probe has been launched).

Expert acousticians are required in such design. Our experience as humans of audiofrequency sound in air (with its limited ranges of amplitude and frequency – Figures 1 and 2) does not equip the non-expert with an intuitive appreciation of the opportunities to exploit acoustics in extraterrestrial solids, liquids and gases, just as it does not equip us intuitively to appreciate how cetaceans exploit acoustics in the oceans (Leighton *et al.*, 2005(a)).

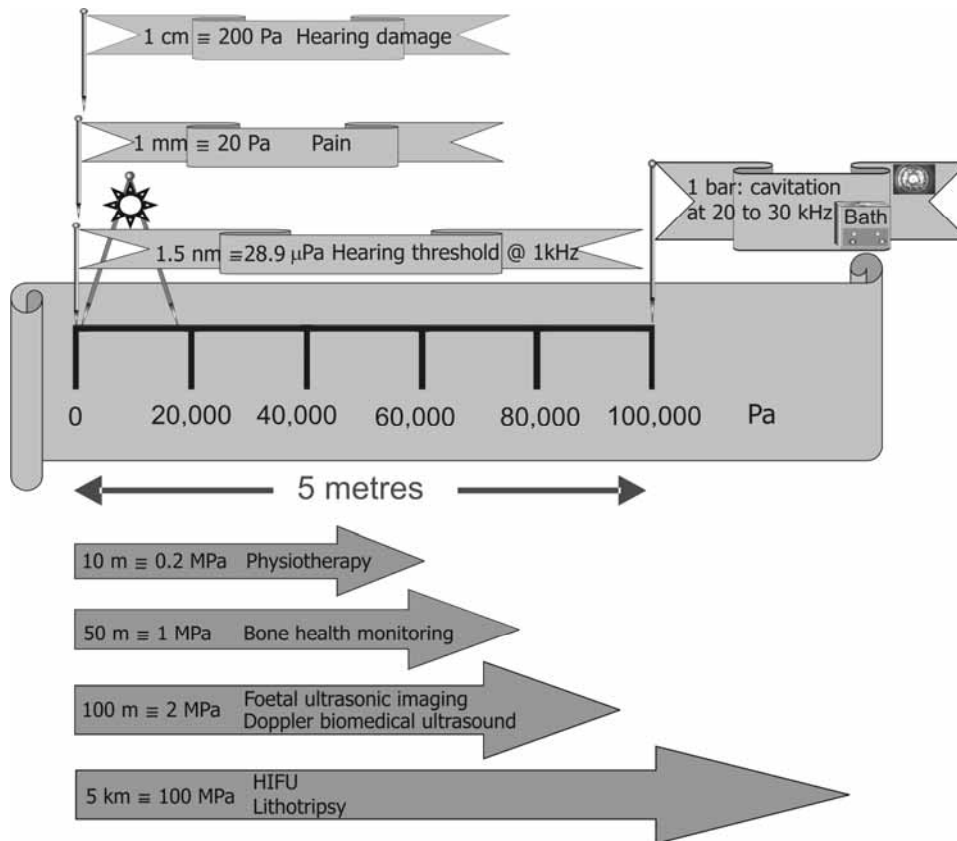


Figure 2. The figure shows several identifiable features on a scale of the acoustic pressure amplitude. It is based on a demonstration of such scales, where five markers (indicating, respectively, 20, 40, 60, 80 and 100 kPa) were placed at 1 m intervals from a datum (representing 0 Pa). The figure illustrates this schematically through an unfurled banner, onto a 5 m section of which are placed the six markers for 0–100 kPa. Human hearing occupies a small part of this range, as indicated by three flags which have been stacked at the top left of the figure because there is not enough space to pin them in their proper places. At 1.5 nm from the datum is placed the pin indicating an acoustic pressure amplitude of 28.9 mPa, taken to be the threshold for hearing at 1 kHz. At 1 mm is placed the pin for an acoustic pressure of 20 Pa, which would cause pain in humans; and at 1 cm is placed the pin for 200 Pa, which would cause hearing damage in normal human ears. A pair of dividers, topped with a sun, is drawn with its points at 300 Pa and 17 kPa. This is done to illustrate the point that, although even the lower point of the dividers (300 Pa) exceeds the threshold for hearing damage, nevertheless the intensities are what physically we might regard as ‘low’. This is because the two point of the dividers correspond to the acoustic pressure amplitudes (in air and water) which would provide in a plane wave the same intensity as daylight. Bright sunshine is considered to be occurring when the solar radiation level exceeds 100 Wm^{-2} (although in actual fact this level would be perceived to correspond to a dull day). Equivalent plane wave intensity occurs in water for zero-peak acoustic pressure amplitudes of 17 kPa in water and 300 Pa in air. The final flag is pinned at the 5 m mark, corresponding to 1 atmosphere of pressure, the threshold for cavitation at low ultrasonic frequencies. Below the scale are arrows indicating tentative values for the acoustic pressure amplitudes which can be measured from a range of biomedical ultrasonic devices operating in degassed water (measurement in vivo in tissue is difficult, but would produce lower values than those that could be generated in degassed water). Additional reasons why these values can only be tentative include the difficulty in assigning pressure amplitudes (to systems shown below the banner) because of the range of waveforms and pulse durations used, the question of whether one refers to the peak positive or peak negative pressure, etc., and because of the acceptable error limits in many ultrasonic measurements. Biomedical applications which are considered to be ‘low intensity’ (physiotherapy, bone health monitoring etc.) occur at respective distances of 10 m and 50 m on this scale (equivalent to acoustic pressure amplitudes of 0.5–1 MPa). Foetal ultrasonic imaging and Doppler biomedical ultrasound are tentatively located at 100 m from the datum on this scale, corresponding to acoustic pressure amplitudes of about 2MPa. The therapeutic applications of HIFU (ultrasonic surgery) and lithotripsy are placed at a range of 5 km on this scale (corresponding to acoustic pressures of 100 MPa). Taken from Leighton (2007).

2 Use of acoustics in extraterrestrial research

The extent to which acoustics *per se* is used in extraterrestrial research varies greatly, and this section provides four broad classifications.

2.1 Construction of artificial acoustic time-series

At one end of the range of these studies, sound is simply used as the medium through which some other time-varying non-acoustic signal (such as radio waves generated by Jovian lightning) is communicated to humans. See for example the material at <http://www-pw.physics.uiowa.edu/space-audio/>. At the other end of this range, there may have been some acoustical perturbations involved in the generation of the signal, and some justification therefore for attributing a degree of meaning to an acoustical representation, although often the degree of integrity with which the measured signal reflects the original acoustical perturbation is often untestable. An example of this, which might from some perspectives more properly be classed as belonging to section 2.2, can be found in the construction of an audio signal from the fluctuations in the cosmic background radiation which are thought to be related to acoustical fluctuations in the early expanding universe 14 billion years ago (De Bernardis *et al.*, 2000; Cramer, 2001; Bento, 2003); see <http://staff.washington.edu/seymour/altvw104.html>.

2.2 Interpretation of perturbations in other radiations by appealing to acoustical fluctuations at source

Studies of the type mentioned at the end of section 2.1 form the link to investigations whereby perturbations in a non-acoustic signal (e.g. EM) are interpreted through mechanisms relating to acoustic perturbations in the source material itself. These traditional extraterrestrial acoustical investigations have been dominated by the use of models of infrasonic waves in order to interpret perturbations in EM data. Examples include modal acoustic waves in planets (Lee, 1993) and stars (Noyes *et al.*, 1997; Bouchy *et al.*, 2005), which may for example identify the existence of planets or, in our own solar atmosphere, to investigate solar dynamics (Elsworth *et al.*, 1990; Rammacher and Ulmschneider, 1992); and in dust plasmas such as occur in planetary rings, comets and noctilucent clouds (Verheest, 1993; Pieper and Goree, 1996; Rosenberg and Kalman, 1997; Merlino, 1997; Shukla, 2000, Gupta *et al.*, 2001).

2.3 Measurement of acoustic signals introduced by the probe itself

Some probes have made direct measurements of acoustic signals which have been generated by the probe itself. This might be done, for example, to infer the local atmospheric sound speed from the time-of-flight of an acoustic pulses over a short distance ($O(10\text{ cm})$).

Such direct acoustical observations are understandably rarer than the investigations discussed in section 2.2, because of the need successfully to deploy a probe and receive viable transmissions. With an appropriate propagation model, the received acoustic signal can be interpreted (inverted) to estimate the properties of the source and the propagation path. For probes which transmit and receive artificially-generated acoustic pulses, the source is well-known and the interpretation reveals details of the propagation medium. This might range from inferring atmospheric sound speed from time-of-flight measurements over a few cm (Lebreton *et al.*, 2005) to, speculatively, propagation around entire planets (Leighton *et al.*, 2006, 2007).

2.4 Construction and inversion of the acoustical soundscape

Section 2.3 discussed the detection, by a microphone on a probe, of acoustic pulses which were generated by the probe itself. Given that the characteristics of the source are well-known, the inversion is based on (and seeks to determine) the unknown parameters of the medium through which the acoustic pulse propagated.

If the source of sound is natural (in that the microphone, hydrophone or geophone detects an extraterrestrial acoustic signal), the power requirements and complexity of the hardware in principle become simpler. However the inversion discussed above now contains an extra cause of uncertainty (i.e. the characteristics of the source), making it a much more demanding task for anything more than a rudimentary characterisation of the sound source (e.g. distinguishing between lightning and self-noise in the probe).

Some probes have carried microphones (Ksanfomality *et al.*, 1983(a,b); Lebreton *et al.*, 2005), and there have been spectacular successes from such missions in collecting data from a wide range of sensors (Zarnecki *et al.*, 2005; Tokano *et al.*, 2006; Stofan *et al.*, 2007). However there are as yet (to the author's knowledge) no published results of in-depth interpretation and inversion of the natural acoustical signals generated by the extra-terrestrial environment in order to characterise that environment (Fulchignoni *et al.*, 2005(a,b), 2006; The Planetary Society, 2007).

Nevertheless our understanding of acoustics is sufficient not only to predict the natural acoustic surrounding (including the soundscape which would be audible to human hearing), but also is able to present methods of how acoustic data might be quantitatively inverted to characterise the environment (Leighton, 2004; Leighton and White, 2004; Leighton *et al.*, 2005(b), 2006).

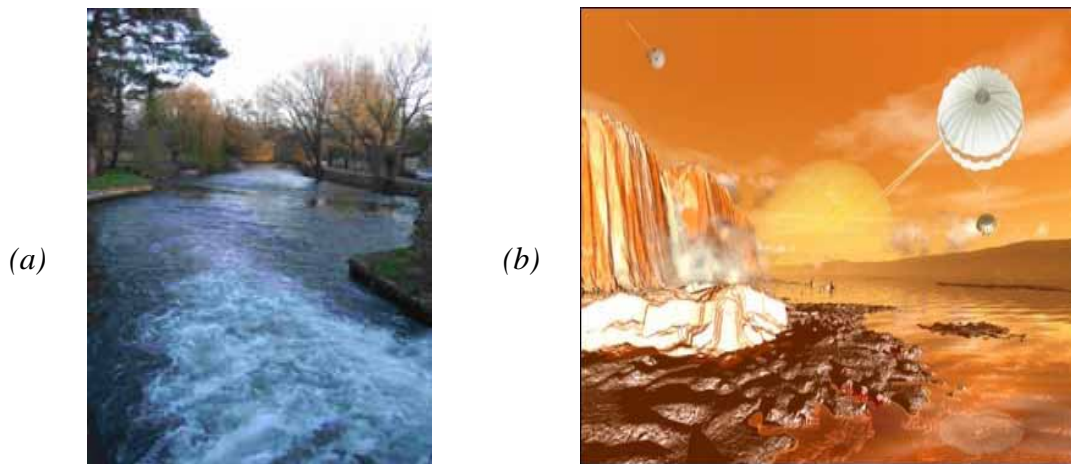


Figure 3. (a) The Salmon Leap, Sadler's Mill, Romsey (Longitude 1°30' W; Latitude 50° 59'N). View to the South-south-west, looking downstream towards the Broadlands estate. The hydrophone was placed at a depth of 10 cm in clear water, about 3 m from the turbulent bubble cloud. (Photograph: T G Leighton). (b) An artist's impression of Titan's surface, undertaken prior to the mission landing. In the sky, Saturn is visible dimly in the background through Titan's thick atmosphere. The Cassini spacecraft flies over the surface with its High Gain Antenna pointed at the Huygens probe as it nears the end of its parachute descent. Thin methane clouds dot the horizon, and a narrow methane spring or "methanefall" flows from the cliff at left and produces considerable vapour. Smooth ice features rise out of the methane/ethane lake, and crater walls can be seen far in the distance. (Illustration by David Seal, Image credit: NASA/JPL/Caltech).

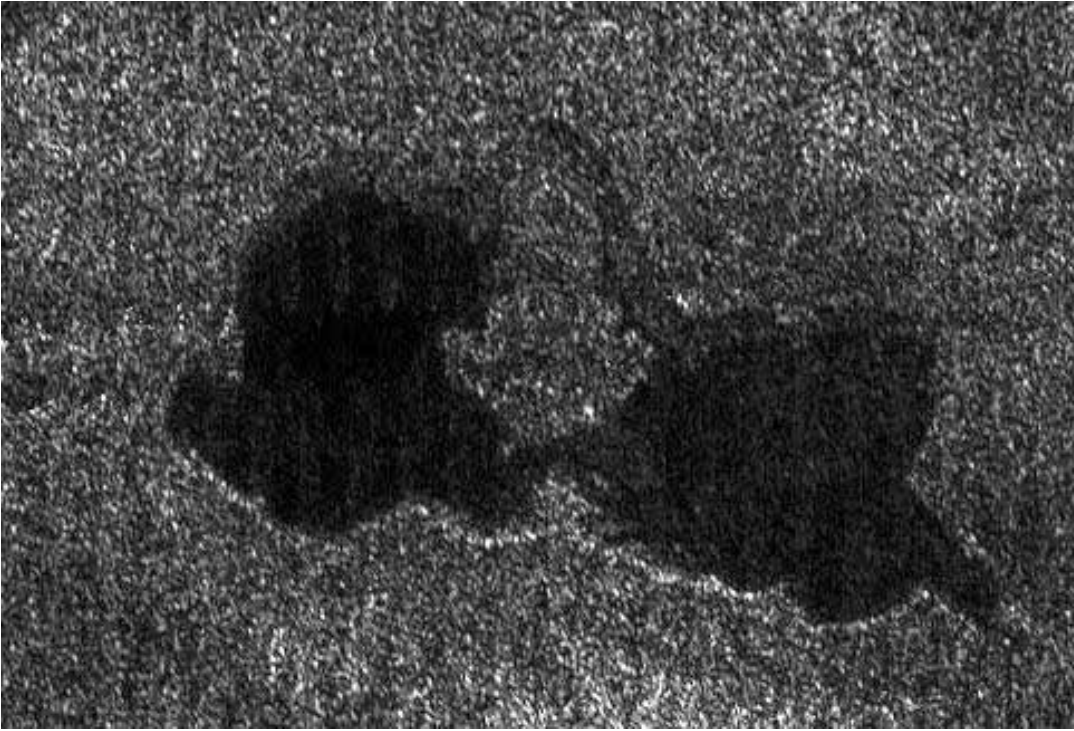


Figure 4. In this Cassini radar image, two of Titan's lakes (near 73 degrees north latitude, 46 degrees west longitude) are seen, each 20 to 25 kilometers (12 to 16 miles) across. The image from a flyby on Sept. 23, 2006, covers an area about 60 kilometers (37 miles) wide by 40 kilometers (25 miles) high. They are joined by a relatively narrow channel. The lake on the right has lighter patches within it, indicating that it may be slowly drying out as the northern summer approaches. This image is provided courtesy of NASA/JPL.

Prior to the landing of the Huygens probe on Titan, the existence or otherwise of free-flowing liquid on the moon's surface was controversial¹. Leighton and co-workers developed a physical model for the way sounds are developed by impacts of bodies (including water droplets) travelling through an atmosphere with liquid, and used them to invert the sound of a terrestrial waterfall (Figure 3(a)) and the splashdown of a Huygens probe mimic to determine the key values for the parameters responsible for those sounds. These values were then adapted for the postulated 'waterfalls' (actually, 'methanefalls') and lakes on Titan, and ran the 'forward problem' to predict the sounds of a methanefall (Figure 3(b)) and a splashdown on Titan, should Huygens encounter either (Leighton, 2004; Leighton and White, 2004; Leighton *et al.*, 2005(b), 2006). These sounds are available via the labelled link on <http://www.isvr.soton.ac.uk/fdag/uaua.HTM>.

The most recent evidence from Titan (Sotin, 2007; Stofan *et al.*, 2007) suggests that lakes do in fact exist in a number of states (Figures 4 to 6), including partly dry and liquid-filled, which (when

¹ In the same year that the soundscape was published for Leighton and White (2004), *New Scientist* stated that "Titanic waves break on Saturn's sludgy moon" (31 March 2004) and then, on 10 November 2004 a lack of mirror-like reflections for camera and radar on Cassini (altitude 12,000 km, 4 locations) prompted the *New Scientist* headline "Titan has no breaking waves".

added to earlier evidence that flowing liquid has existed in the moon's surface (Figure 7)) reinforces a picture of a world with liquid open to an atmosphere.



Figure 5. This side-by-side image shows a Cassini radar image (on the left) of what is the largest body of liquid ever found on Titan's north pole, compared to Lake Superior (on the right). This close-up is part of a larger image and offers strong evidence for seas on Titan. These seas are most likely liquid methane and ethane. This feature on Titan is at least 100,000 square kilometers (39,000 square miles), which is greater in extent than Lake Superior (82,000 square kilometers or 32,000 square miles), which is one of Earth's largest lakes. The feature covers a greater fraction of Titan than the largest terrestrial inland sea, the Black Sea. The Black Sea covers 0.085 percent of the surface of the Earth; this newly observed body on Titan covers at least 0.12 percent of the surface of Titan. Because of its size, scientists are calling it a sea. The image on the right is from the SeaWiFS project, NASA's Goddard Space Flight Center, Greenbelt, Md. (Image Credit: NASA/JPL/GSFC).

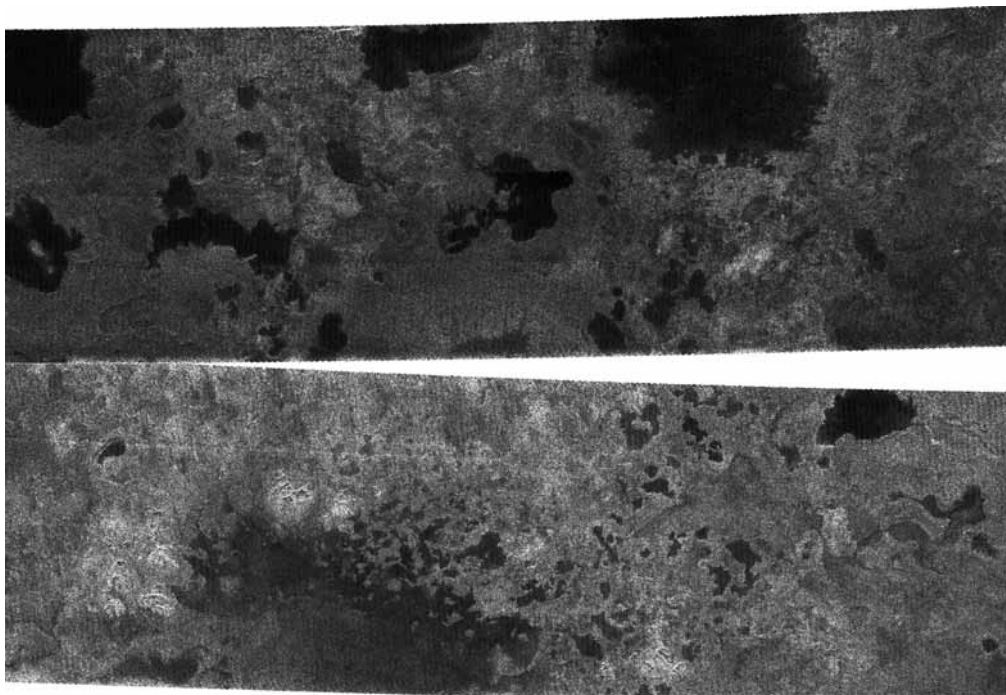


Figure 6. These two radar images were acquired by the Cassini radar instrument in synthetic aperture mode on July 21, 2006. The top image centred near 80 degrees north, 92 degrees west measures about 420 km by 150 km (260 miles by 93 miles). The lower image centred near 78 degrees north, 18 degrees west measures about 475 km by 150 km (295 miles by 93 miles). Smallest details in this image are about 500 meters (1,640 feet) across. The variety of dark patches in the image suggest the presence of many lakes in the high latitudes around the North Pole of Titan. Some of these dark patches have channels leading in or out of them. The channels have a shape that strongly implies they were carved by liquid. Some of the dark patches and connecting channels are completely black, that is, they reflect back essentially no radar signal, and hence must be extremely smooth. In some cases rims can be seen around the dark patches, suggesting deposits that might form as liquid evaporates. Because such lakes may wax and wane over time, and winds may alter the roughness of their surfaces, repeat coverage of these areas should test whether these are indeed bodies of liquid. (Image Credit: NASA/JPL).

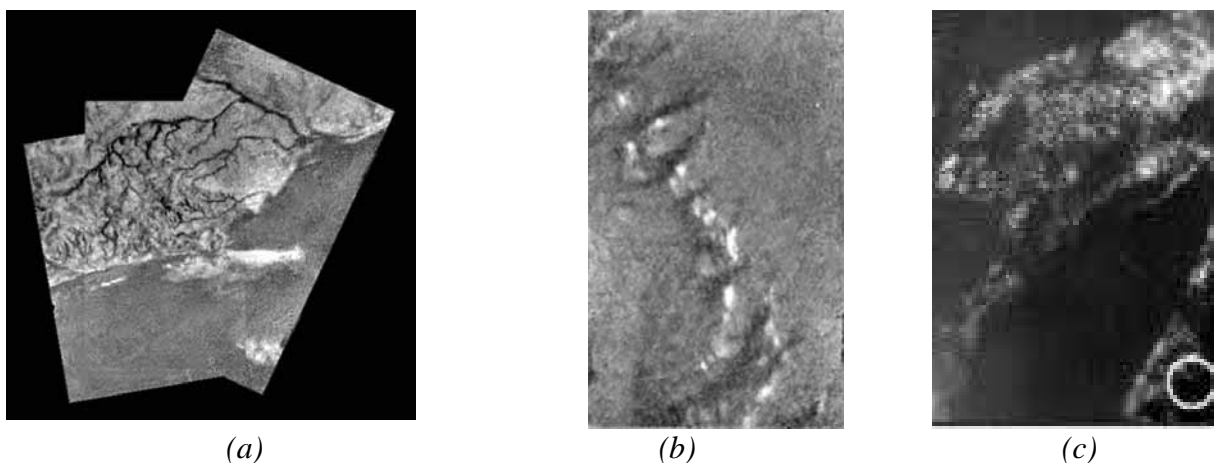


Figure 7. Images of Titan obtained by the Huygens probe. (a) This mosaic of three frames provides detail of a high ridge area including the flow down into a major river channel from different sources. (b) A single image from the Huygens DISR instrument of a dark plain area on Titan, seen during descent to the landing site. There appears to be flow around bright 'islands'. The areas below and above the bright islands may be at different elevations. (c) The landing site of Huygens is circled. (Credits: ESA/NASA/JPL/University of Arizona).

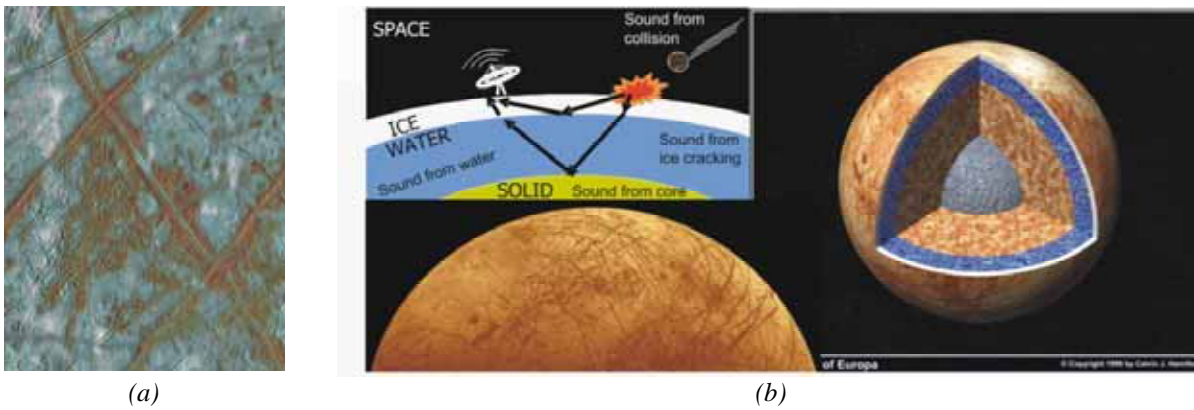


Figure 8. (a) Cracks on Europa's ice surface. Most scientists believe that salts and other inorganic materials are responsible for the coloured patches on Europa's outer layer, although there has been speculation that bacteria, extruded through the ice from below and 'flash frozen' on the surface, are responsible. (Credit: NASA/JPL) (b) Top left: schematic of possible acoustic-based mission to Europa, where acoustic signals originating from various planetary sources are passively detected and transmitted to Earth via an orbiter (schematic: TG Leighton). Lower: the surface of Europa, showing ice features (Credit: NASA/JPL). Right: Schematic of the interior of Europa, showing ice covering over a water ocean, overlaying the solid interior (Copyright Calvin J Hamilton).

Several notable acoustical investigations feature Europa, a main objective being exploration of ways to characterise the ocean which could be present beneath the surface ice (Figure 8). Kovach and Chyba (2001) produced pioneering studies which modelled acoustic propagation in the ice. They described how a seismometer on Europa could passively detect surface waves propagating in the frequency band of 0.1 to 0.5 Hz (having wave periods of 2 to 10 s). They described how such 'signals of opportunity' could be used to determine the presence or absence of a possible sub-ice ocean and, furthermore, how they could be interpreted to provide estimates of the ice thickness. The list of candidate 'signals of opportunity' includes ice fractures (Hoppa *et al.*, 1999) and comet and asteroid impacts (Zahnle *et al.* 1998) (see inset in Figure 8(b)). Lee *et al.* (2003) developed such studies to consider acoustic propagation in both the ice and the sub-ice ocean of Europa. These investigations opened the way for assessing Europa's ice and ocean using acoustical signals of opportunity, generated by natural processes in the ice, ocean or mantle (Crawford and Stevenson, 1988; Schenk and McKinnon, 1989; Hoppa *et al.*, 2000; Greenberg, 2002; Lee *et al.*, 2005; Nimmo and Schenk, 2006; Panning *et al.*, 2006; Leighton *et al.*, 2006, 2007). Understandably, such studies require assumptions to be made about the extraterrestrial environment which are often based on remote observation and therefore contain uncertainties. For example, in the case of Europa these assumptions may pertain to the salinity (Khurana *et al.* 1998; Kivelson *et al.*, 2000), temperature (Melosh *et al.*, 2004) and depth (Pappalardo *et al.*, 1998) of the proposed ocean.

In order to find the required propagation model for acoustic inversion, it is efficient to transpose our well-established terrestrial models to these off-world environments (Lee *et al.*, 2003). However this needs to be done with care, since the assumptions on which terrestrial models are based may not

hold on other worlds (Leighton *et al.*, 2007). Whilst for example the use of spherical geometry is obvious when one is dealing with such whole-body acoustics as the oscillatory modes of planets (Lee, 1993) and stars (Elsworth *et al.*, 1990; Rammacher and Ulmschneider, 1992; Noyes *et al.*, 1997; Bouchy *et al.*, 2005), and if one is considering the propagation of acoustic signals (for example from the impact of a comet or asteroid) right around the planet (Leighton *et al.*, 2006, 2007), when propagation over smaller distances ($O(100 \text{ km})$) are considered, the effects of planet curvature may or may not be significant, and should be quantitatively tested (Leighton *et al.*, 2007).

3 Conclusions

Electromagnetic data which has been perturbed at source by acoustical fluctuations will continue to be gathered. Its interpretation will be most efficient if it applies the best available methods in acoustics, as these develop.

The issue of the use of acoustic sensors on probes is perhaps more serious. Discussing the <\$100,000 component of the \$165 million Mars Polar Lander that was spent on providing it with a microphone, Clark (1999) commented that that:

“NASA didn't pay anything for the microphone, which is essentially a welcome stowaway aboard the spacecraft...."It kind of occupies a unique niche between public relations and unique science," said Greg Delory, a research scientist who helped build the microphone at the University of California at Berkeley's Planetary Sciences Laboratory. "It should really raise the level of public interest in the mission."..... its signals may help mission controllers learn how the lander is performing by providing a sort of diagnostic indicator for spacecraft engineers, Delory said. For instance, listening to the sound of solar panels deploying, engineers may be able to tell whether the panels unfold correctly. They will also be able to listen to the sounds of the lander's cameras and hear the robotic arm cut into the crusty layers of the polar surface...Although it is not performing any critical science role, Delory said he expects the mic will help scientists learn something startling about the planet”.

The achievements of those scientists and engineers who deliver any viable signal from a space probe are enormous and should not be underrated. For the reasons outlined in section 1, there is a general tendency amongst public and sponsors to underestimate the specific level of expertise and investment required for acoustics. Those involved in the planning and development of probes should beware of giving the impression that one may treat acoustics as an inexpensive add-on. This risks compromising the ability of acoustics to deliver its best and most reliable information. The

field of sonochemistry provides a salutary example. In the author's experience through the last several decades, there has never been a time when some researchers studying the ability to enhance or promote chemical reactions by applying acoustic fields, have not stated that we are on the verge of an age of massive industrial exploitation of this technology. However the continual absence of such a promised age has a reputation for inability to scale-up, and such unreliability that it is sometimes called a 'black art' (Mason *et al.*, 1992). This has arisen because the vast majority of sonochemistry experiments have been undertaken by chemists without the input of acousticians (Leighton, 2004, 2007). This reputation has in turn compromised the faith of potential sponsors and young researchers in the potential to exploit ultrasound to enhance chemical reactions, to the detriment of the field. Figure 9 illustrates an example of how this situation has come about. In recent years there have been many papers investigating which is the 'best' frequency for a given ultrasonic processing application, undertaken by chemists who 'spot-check' the sonochemical yield generated at a half-a-dozen frequencies covering the range 20 kHz to over 1 MHz (Mark *et al.*, 1998; Hung and Hoffmann, 1999; Sato *et al.*, 2000; Kojima *et al.*, 2001; Becket and Hua, 2001). Such approaches do not convey the message that, because net frequency response of the system is dependent on the frequency responses of several particular pieces of apparatus, the results could be highly laboratory-specific. Instead the impression is given that the reaction itself is responsive only to the timescale of the acoustic local pressure perturbation, an effect which is difficult to reproduce on other apparatus in other laboratories for the following reason. That is, specifically, that in most cases the effect is more sensitive to the spatial peak acoustic pressure amplitude of the inhomogeneous acoustic field². It is therefore only indirectly sensitive to the frequency of the driving field because of the frequency response of the amplification and transduction stages and, crucially, of the specific vessel in which the liquid chemical sample is contained (Leighton, 2007).

² There are, of course, direct influences from the acoustic frequency through for example the cavitation threshold, but these are secondary to the influence of the spatial peak acoustic pressure amplitude.

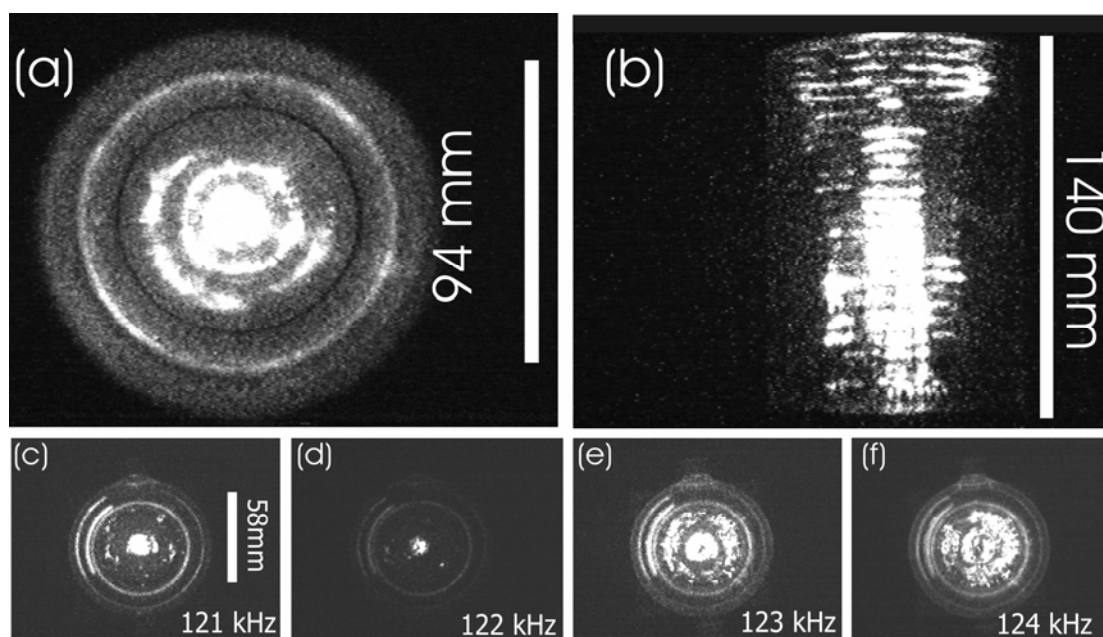


Figure 9. The acoustic pressure antinodes within cylinders filled with aqueous solution (with vertical axis of symmetry, and the sound source at the cylinder base) are made visible through the chemiluminescence which occurs there. (a) Plan and (b) side views of luminescence (which occurs at pressure antinodes) in a liquid-filled cell which had a polymethylmethacrylate wall (9.4 cm internal diameter, 10 cm external diameter; height of aqueous solution=14 cm) for insonification at 132.44 kHz where the spatial peak acoustic pressure in the liquid was 75 kPa (all quoted zero-to-peak). Frames (c)-(f) (to which the scale bar of length 5.8 cm in frame (c) refers) were taken in a double-walled, water-jacketed cell (5.8 cm internal diameter, 8.5 cm external diameter, and liquid height 8 cm) which was maintained at a constant liquid temperature of 25°C. For a constant applied drive voltage, as the insonifying frequency changed, so too did the spatial peak acoustic pressure, providing the following combinations: (c) 121 kHz; 139 kPa; (d) 122 kHz; 150 kPa; (e) 123 kHz; 180 kPa; (f) 124 kHz; 200 kPa. The effect of tuning into particular acoustic modes is evident: a 1 kHz change in frequency can dramatically alter the amount and distribution of the luminescence (Birkin *et al.*, 2003(a,b)). Hence the not uncommon practice of incrementing frequencies by O(100 kHz) when testing for the ‘optimal processing frequency’ in such arrangements is nonsensical. Similarly, if calorimetry were used to estimate the ultrasonic field, the change of sound speed resulting from the rise in liquid temperature could detune the mode. By noting the modal resonance frequencies in these and similar cylinders, the sound speed in this bubbly water was found to be in the range 868-1063 m/s, implying void fractions of $2.9\text{-}4.2 \times 10^{-3}$ %. Frames selected from several figures in Birkin *et al.* (2003(a)). (Figure including data from P.R. Birkin, J.F. Power, T.G. Leighton and A.M.L. Vincotte; taken from Leighton, 2007).

As a specific example, Figure 9 uses the chemical luminescence generated by the action of the sound field to indicate not only the amount of sonochemical activity, but also its location. The experiment, as is usually the case in such tests, is undertaken in a cylindrical vessel, with its axis vertical. At certain frequencies the sound field can stimulate acoustic modes in the vessel, which take the form of Bessel functions when viewed from above (Figures 9(a), (c)-(f)), and plane standing waves when viewed from the side (Figure 9(b)). The results of Figure 9 show that a change of 1 kHz (<1% of the driving frequency) can dramatically change the chemiluminescence produced by the acoustic field (Birkin *et al.*, 2003(a,b)): in such a system, spot-checking the chemical activity at half-a-dozen frequencies spaced 10s or even 100s of kHz apart would provide a experiment-specific result for the ‘best’ frequency, dependent on the dimensions of the vessel and indeed the depth of liquid to which it is filled. Publishing an ‘optimal’ frequency for a given reactions will inevitably lead to a failure to replicate the effect in another laboratory if other equipment is used.

The result of not understanding the complexity of the acoustics can lead to poor performance; and when it appears to be inexpensive to produce results, the literature becomes dominated by so many irreproducible results that more thorough proposals appear to be overpriced. Furthermore, when poor performance and low expectations become the accepted norm for a field, rigorous studies can seem anomalous and outweighed by ‘received wisdom’.

There are by no means enough acoustic studies yet in space exploration to lead to such a state of affairs. However the statements made by the community must not give the impression that this is the route they follow. The quote above suggests an expectation for low investment. Acoustic information is more than a public-awareness tool, and its interpretation can be far more sophisticated than ‘does it, or does it not, sound like thunder?’. When faced with a stranger, the visual image can tell you their sex and age, but the acoustic information can tell you what they are thinking about, and possibly where they were born. With the understandably massive investment that has gone into equipping probes to transmit images, the balance of resources available for acoustic information should be addressed. The abilities of acoustic sensors on probes should not be underestimated. They can not only provide complementary data to existing systems, but to do so at comparatively little extra cost and with rugged, light-weight equipment. Furthermore, their ability to exploit signals of opportunity in a passive manner has vast implications. Not only is it efficient in terms of power usage, but it examines a signal generated by the extraterrestrial environment itself. With the rapidly increasing abilities of acousticians to invert such signals, acoustics perhaps offers far more opportunities than were anticipated. As probes are designed to explore new environments, acoustic sensors should represent more than the detection of (primarily turbulent, as opposed to acoustic) pressure fluctuations as the probe travels through the gaseous matter of planets, moons and comet tails. They should also represent the possibilities inherent in the infrasonic and the ultrasonic regimes, and be designed to exploit valuable information from the acoustic propagation that can occur in solids, liquids and plasmas. The range of sensors available extends wider than the electret microphone, to hydrophones and geophones capable of withstanding the pressure of the sea bottom or the conditions within a drill hole.

Acoustic propagation requires two components: inertia, and a restoring force³ which acts in response to displacement, such that mechanical energy can be stored and propagate in the medium. These components occur in many media throughout the solar system (and beyond), including planetary rings (Figure 10), atmospheres (Figure 11), oceans (Figure 8), solar coronas (Figure 12),

³ Such forces can arise from a wide variety of origins, from stiffness in a solid to gravitational forces in a gas.

the solar wind, dust clouds, comet tails (Figure 13) and the solid matter of the various bodies in the solar system (Figure 9 and Figure 14). With the option both of remote sensing of acoustic waves and of their direct measurement using probes, and the wealth of discontinuous process (e.g. impact (Figure 11 and Figure 15), detachment (Figure 13) and geophysical activity) which can provide sources of opportunity, the opportunities for acoustical exploration of space are many.

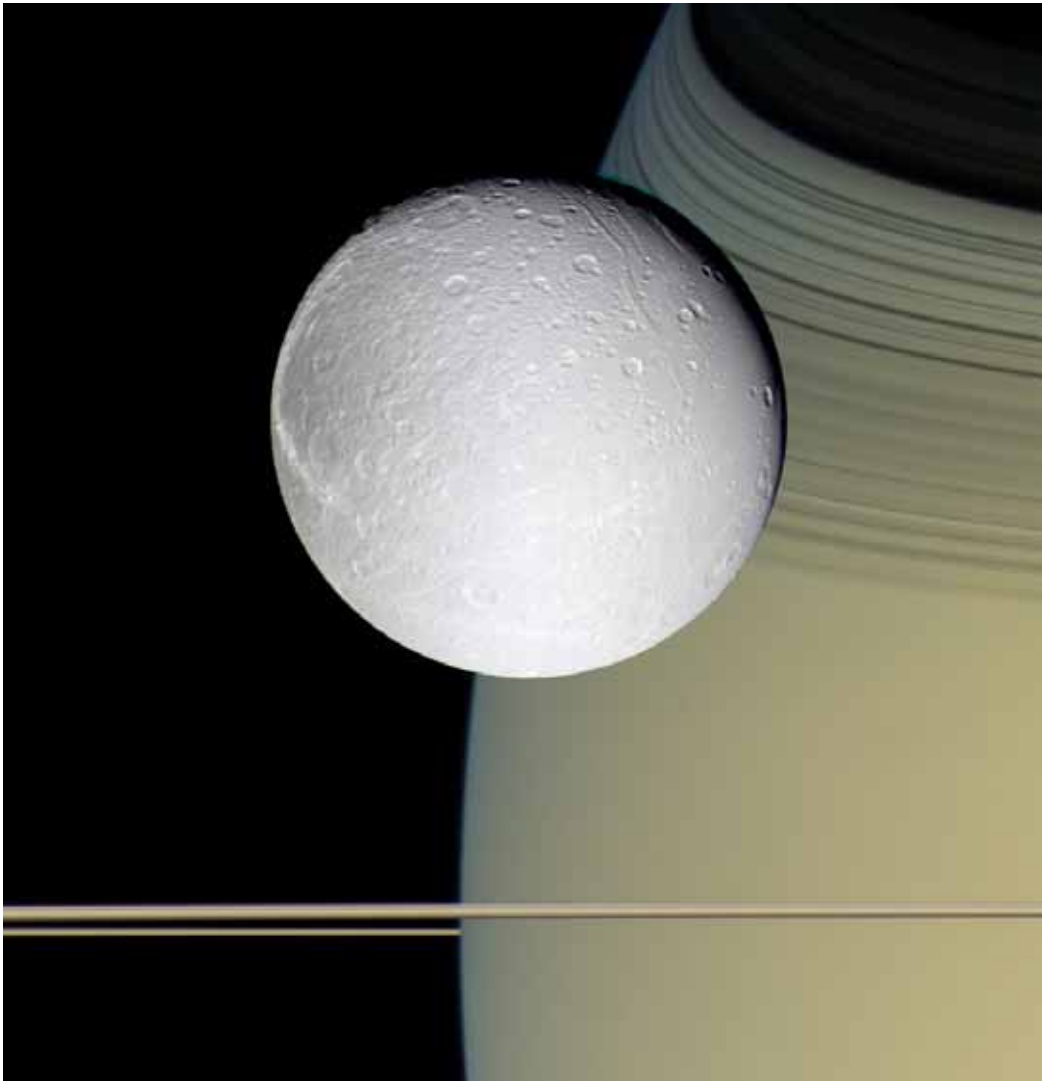


Figure 10. Images taken on Oct. 11, 2005 using the Cassini spacecraft wide-angle camera at a distance of approximately 39,000 kilometers (24,200 miles) from Dione and at a Sun-Dione-spacecraft angle of 22 degrees. The image scale is about 2 kilometers (1 mile) per pixel. The camera employed blue, green and infrared (centred at 752 nanometers) spectral filters, which were used to create this colour view, which approximates the scene as it would appear to the human eye. Speeding toward pale, icy Dione, Cassini's view is enriched by the tranquil gold and blue hues of Saturn in the distance. The horizontal stripes near the bottom of the image are Saturn's rings. The spacecraft was nearly in the plane of the rings when the images were taken, thinning them by perspective and masking their awesome scale. The thin, curving shadows of the C ring and part of the B ring adorn the northern latitudes visible here, a reminder of the rings' grandeur. It is notable that Dione, like most of the other icy Saturnian satellites, looks no different in natural color than in monochrome images. (Image Credit: NASA/JPL/Space Science Institute).



Figure 11. This ultraviolet image taken from the Hubble Space Telescope shows Jupiter's atmosphere after many impacts by fragments of comet Shoemaker-Levy 9. A large, dark patch from the impact of fragment H is visible rising on the left side. Proceeding to the right, other dark spots were caused by impacts of fragments Q1, R, D and G, and L, with L covering the largest area of any seen thus far. The spots are very dark in the ultraviolet because a large quantity of dust is being deposited high in Jupiter's stratosphere, and that dust absorbs sunlight. Scientists will be able to track winds in the stratosphere by watching the evolution of these features. Jupiter's moon, Io, is the dark spot just above the center of the planet. (Image Credit: Credit: Hubble Space Telescope Comet Team).

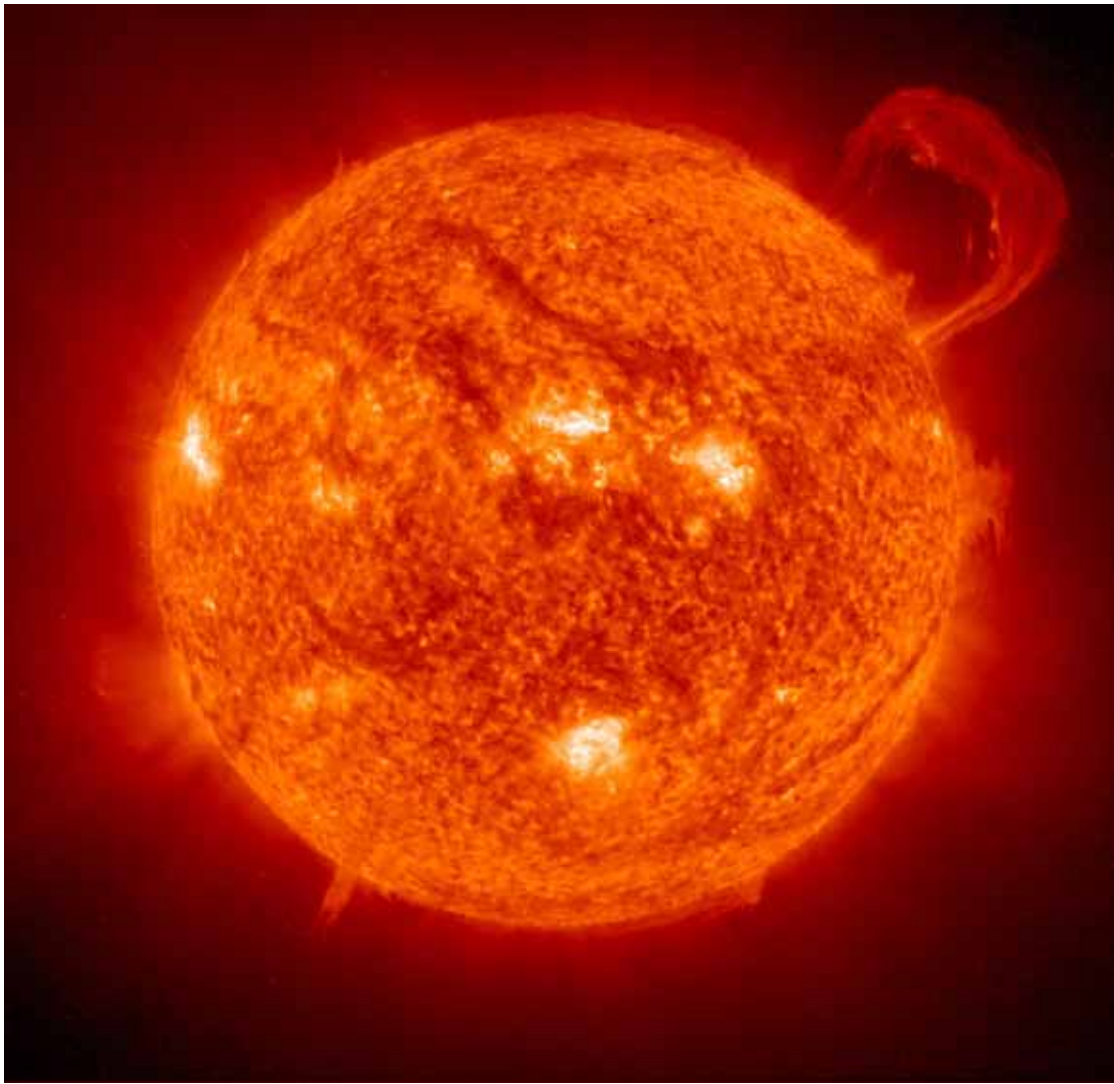


Figure 12. Extreme Ultraviolet Imaging Telescope (EIT) image of a huge, handle-shaped prominence taken on Sept. 14, 1999 taken in the 304 angstrom wavelength. Prominences are huge clouds of relatively cool dense plasma suspended in the Sun's hot, thin corona. At times, they can erupt, escaping the Sun's atmosphere. Emission in this spectral line shows the upper chromosphere at a temperature of about 60,000 degrees K. Every feature in the image traces magnetic field structure. The hottest areas appear almost white, while the darker red areas indicate cooler temperatures. (Image Credit: Courtesy of SOHO/Extreme Ultraviolet Imaging Telescope (EIT) consortium).

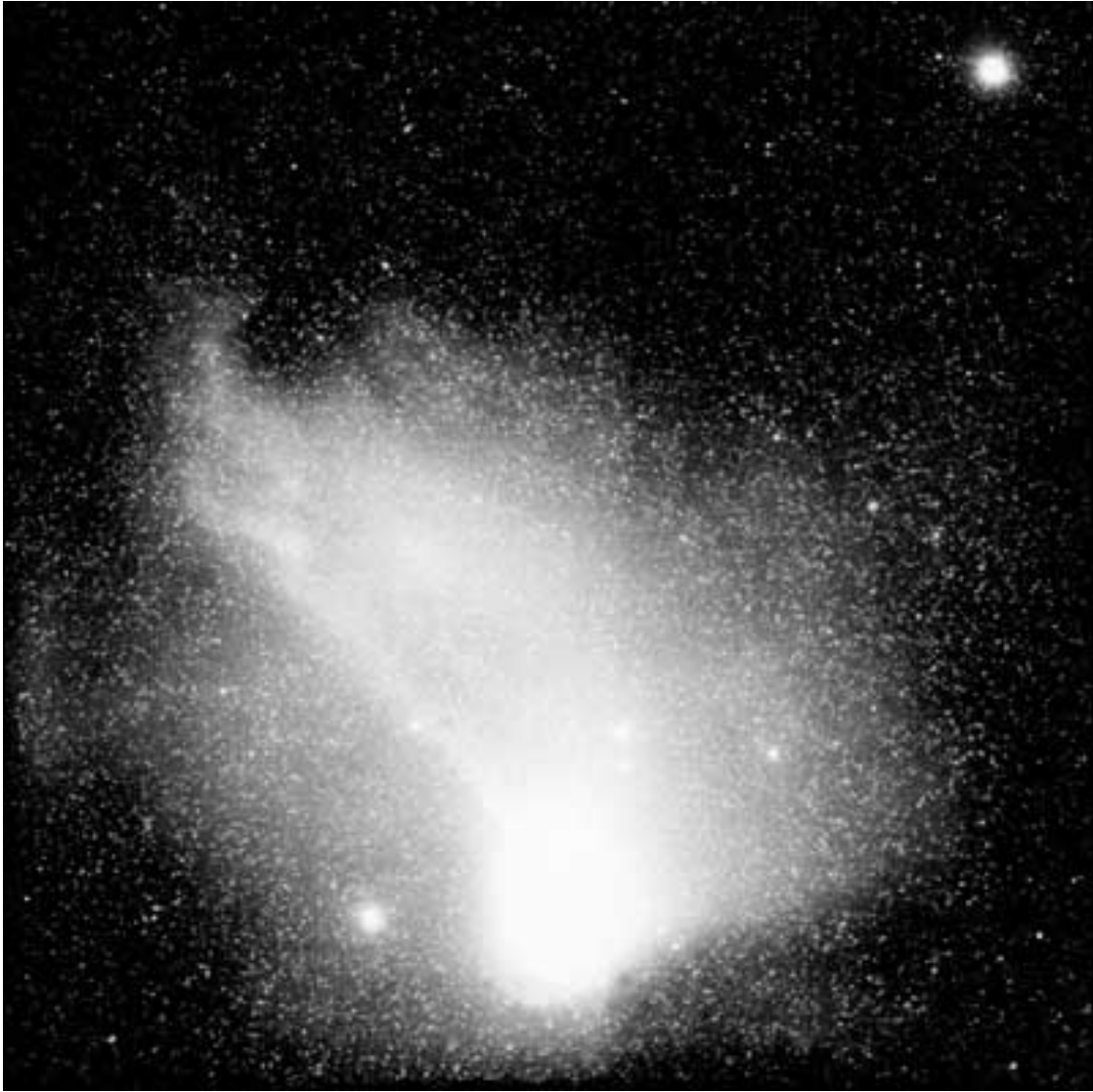


Figure 13. One of the more spectacular changes recorded for Halley during an apparition was the detachment event that happened April 12, 1986. This 3-minute exposure was taken using the Michigan Schmidt telescope at Cerro Tololo Interamerican Observatory. The resulting image clearly shows part of the ion tail structure detached from the comet. At this period, the orientation of the comet is such that the tail is foreshortened, with the prolonged radius vector pointing west of north. (Image credit: NASA/JPL).



Figure 14. Gullies in Sirenum Terra, Mars (Date: 10.03.2006). This enhanced-color view shows gullies in an unnamed crater in the Terra Sirenum region of Mars. It is a sub-image from a larger view imaged by the High Resolution Imaging Science Experiment (HiRISE) camera on NASA's Mars Reconnaissance Orbiter on Oct. 3, 2006. This scene is about 254 meters (about 830 feet) wide. The upper and left regions of this scene are in shadow, yet colour variations are still apparent. The high signal to noise ratio of the HiRISE camera allows for colours to be distinguished in shadows. This allows dark features to be identified as true albedo features versus topographical features. (Image credit: NASA/JPL/Univ. of Arizona).

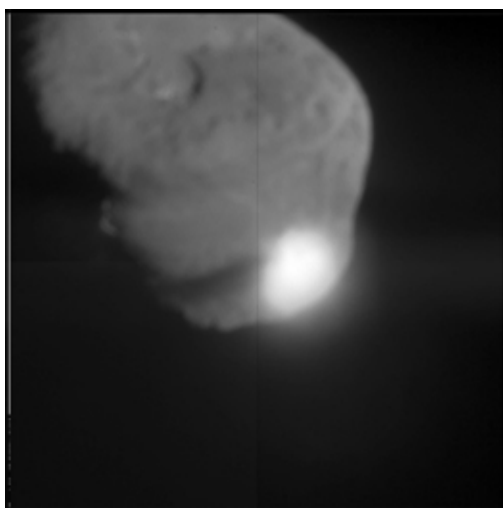


Figure 15. When NASA's Deep Impact probe collided with Tempel 1, a bright, small flash was created, which rapidly expanded above the surface of the comet. This flash lasted for more than a second. After the initial flash, there was a pause before a bright plume quickly extended above the comet surface. The debris from the impact eventually cast a long shadow across the surface, indicating a narrow plume of ejected material, rather than a wide cone. The Deep Impact probe appears to have struck deep, before gases were heated and explosively released. The impact crater was observed to grow in size over time. A preliminary interpretation of these data indicate that the upper surface of the comet may be fluffy, or highly porous. The observed sequence of impact events is similar to laboratory experiments using highly porous targets, especially those that are rich in volatile substances. The duration of the hot, luminous gas phase, as well as the continued growth of the crater over time, all point to a model consistent with a large crater. This image was taken by Deep Impact's medium-resolution camera. (Image credit: NASA/JPL-Caltech/UMD).

References

- Becket, M.A., Hua, I., 2001. Impact of Ultrasonic Frequency on Aqueous Sonoluminescence and Sonochemistry. *Phys. Chem. A*, 105, 3796-3802.
- Bento, M. C., Bertolami, O., Sen, A. A., 2003. Generalized Chaplygin gas and cosmic microwave background radiation constraints, *Phys. Rev. D* **67**, 063003-1 to 063003-5.
- Bouchy, F., Bazot, M., Santos, N. C., Vauclair, S., Sosnowska, D., 2005. *Asteroseismology of the planet-hosting star μ Arae. I. The acoustic spectrum. Astronomy and Astrophysics*, **440**, 609-614.
- Birkin, P.R., Leighton, T.G., Power, J.F., Simpson, M.D., Vincotte, A.M.L., Joseph, P.F., 2003(a). Experimental and theoretical characterisation of sonochemical cells. Part 1: Cylindrical reactors and their use to calculate speed of sound. *J. Phys. Chem. A*, **107**, 306-320.
- Birkin, P.R., Power, J.F., Vincotte, A.M.L., Leighton, T.G., 2003(b). A 1kHz resolution frequency study of a variety of sonochemical processes, *Phys Chem Chem Phys*, **5**, 4170-4174.
- Clark, G., 1999. Listening for the Buzz of Thin Windy Air, 991014
http://www.space.com/news/mars_microphone991014.html

- Cramer, J. G., 2001. BOOMERanG and the Sound of the Big Bang, *Analog Science Fiction & Fact Magazine*; Issue 01/01, Article AltVw104 (January 2001).
- Crawford, G. D., and D. J. Stevenson 1988. Gas driven water volcanism in the resurfacing of Europa. *Icarus* **73**, 66–79.
- De Bernardis, P., Ade, P. A. R., Bock, J. J., Bond, J. R., Borrill, J., Boscaleri, A., Coble, K., Crill, B. P., De Gasperis, G., Farese, P. C., Ferreira, P. G., Ganga, K., Giacometti, M., Hivon, E., Hristov, V. V., Iacoangeli, A., Jaffe, A. H., Lange, A. E., Martinis, L., Masi, S., Mason, P. V., Mauskopf, P. D., Melchiorri, A., Miglio, L., Montroy, T., Netterfield, C. B., Pascale, E., Piacentini, F., Pogosyan, D., Prunet, S., Rao, S., Romeo, G., Ruhl, J. E., Scaramuzzi, F., Sforna, D., Vittorio, N., 2000. A flat Universe from high-resolution maps of the cosmic microwave background radiation, *Nature* **404**, 955-959.
- Elsworth, Y., Howe, R., Isaak, G. R. Mcleod, C. P., New, R., 1990. Variation of low-order acoustic solar oscillations over the solar cycle, *Nature* **345**, 322–324.
- Fulchignoni, M.; Ferri, F.; Colombatti, G.; Zarnecki, J. C.; Harri, H. M.; Hamelin, M.; Lopez-Moreno, J. J.; Schwingenshuh, K.; Angrilli, F.; HASI Team; 2005(b). HASI Experiment to Titan, *Bulletin of the American Astronomical Society*, **37**, 621 (abstract only).
- Fulchignoni, M., Ferri, F., Angrilli, F., Ball, A. J., Bar-Nun, A., Barucci, M. A., Bettanini, C., Bianchini, G., Borucki, W., Colombatti, G., Coradini, M., Coustenis, A., Debei, S., Falkner, P., Fanti, G., Flamini, E., Gaborit, V., Grard, R., Hamelin, M., Harri, A. M., Hathi, B., Jernej, I., Leese, M. R., Lehto, A., Lion Stoppato, P. F., López-Moreno, J. J., Mäkinen, T., McDonnell, J. A. M., McKay, C. P., Molina-Cuberos, G., Neubauer, F. M., Pirronello, V., Rodrigo, R., Saggin, B., Schwingenschuh, K., Seiff, A., Simões, F., Svedhem, H., Tokano, T., Towner, M. C., Trautner, R., Withers, P., Zarnecki, J. C., 2005(a), In situ measurements of the physical characteristics of Titan's environment, *Nature* **438**, 785-791.
- Fulchignoni, M., Ferri, F., *et al.* Recent results on Titan from the HASI instrument. *Geophysical Research Abstracts*, **8**, 10178, 2006 (abstract only).
- Greenberg, R. 2002. Tides and the biosphere of Europa. *Am. Sci.* **90**, 48–55.
- Griffiths, G., Fielding, S., Roe, H.S., 2001. Some observations of biophysical interaction in the ocean using high frequency acoustics. In: Leighton, T.G., Heald, G.J., Griffiths, H., Griffiths, G. (Eds.), 'Acoustical Oceanography', *Proceedings of the Institute of Acoustics*, Vol. 23 Part 2. Institute of Acoustics, pp. 189–195.
- Gupta, M. R., Sarkar, S., Ghosh, S., Debnath, M., Khan, M., 2001. Effect of nonadiabaticity of dust charge variation on dust acoustic waves: Generation of dust acoustic shock waves, *Physical Review E*, **63**, 046406-1 - 046406-9.

- Holliday, D.V., 2001. Acoustical sensing of biology in the sea. In: Leighton, T.G., Heald, G.J., Griffiths, H., Griffiths, G. (Eds.), *'Acoustical Oceanography'*, *Proceedings of the Institute of Acoustics*, Vol. 23, Part 2. Institute of Acoustics, pp. 172-180.
- Hoppa, G. V., Tufts, B. R., Greenberg, R., Geissler, P. E. 1999. Formation of cycloidal features on Europa. *Science* **285**, 1899–1902.
- Hoppa, G., Greenberg, R., Tufts, B. R., Geissler, P., Phillips, C., Milazzo, M., 2000. Distribution of strike-slip faults on Europa, *J. Geophys. Res.*, 105, 22, 617–628.
- Hung, H., Hoffmann, M. R., 1999. Kinetics and mechanism of the sonolytic degradation of chlorinated hydrocarbons: Frequency effects. *J. Phys. Chem. A*, 103, 2734-2739.
- Khurana, K. K., Kivelson, M. G., Stevenson, D. J., Schubert, G., Russell, C. T., Walker, R. T., Polansky, C., 1998. Induced magnetic fields as evidence for sub-surface oceans in Europa and Callisto. *Nature* **395**, 777–780.
- Kivelson, M. G., Khurana, K. K., Russell, C. T., Volwerk, M., Walker, R. J., Zimmer, C., 2000. Galileo magnetometer measurements: A stronger case for subsurface ocean at Europa. *Science* **289**, 1340–1343.
- Kojima, Y., Koda, S., Nomura, H., 2001. Effect of ultrasonic frequency on polymerization of styrene under sonication. *Ultrasonics Sonochemistry*, 8, 75-79.
- Kovach, R. L., Chyba, C. F., 2001. Seismic Detectability of a Subsurface Ocean on Europa, *Icarus* **150**, 279–287.
- Ksanfomality, L., Goroschkova, N. V., Khondryev, V., 1983(a). Wind Velocity near the surface of Venus from Acoustic Measurements, *Cosmic Research* 21, 161-167.
- Ksanfomality, L. V., Scarf, E. L. and Taylor, F. 1093(b). The Electrical Activity of the Atmosphere of Venus, in Hunten D M (ed) *Venus*, University of Arizona Press.
- Lebreton, J.P., Witasse, O., Sollazzo, C., Blancquaert, T., Couzin, P., Schipper, A.-M., Jones, J. B. Matson, D. L., Gurbits, L. I., Atkinson, D. H. Kazeminejad, B., Pérez-Ayúcar, M., 2005. An overview of the descent and landing of the Huygens probe on Titan, *Nature* **438**, 758–764.
- Lee, S., Zanolini, M., Thode, A. M., Pappalardo, R. T., Makris, N. C., 2003. Probing Europa's interior with natural sound sources, *Icarus* **165**, 144–167.
- Lee, S., Pappalardo, R. T., Makris, N. C., 2005. Mechanics of tidally driven fractures in Europa's ice shell, *Icarus* **177**, 367–379.
- Lee, U., 1993. Acoustic oscillations of Jupiter, *The Astrophysical Journal*, **405**, 359-374.
- Leighton, T. G., 2004. From seas to surgeries, from babbling brooks to baby scans: The acoustics of gas bubbles in liquids', *International Journal of Modern Physics B*, **18**(25), 3267-3314.
- Leighton, T. G., 2007. What is ultrasound? *Progress in Biophysics and Molecular Biology*, **93**, Issues 1-3 , 3-83.

- Leighton, T. G., White, P. R., 2004. The sound of Titan: a role for acoustics in space exploration. *Acoustics Bulletin* **29**, 2004, 16-23.
- Leighton, T. G., Heald, G. G., 2005. "Chapter 21: Very high frequency coastal acoustics," in *Acoustical Oceanography: Sound in the Sea*, H. Medwin, Ed. Cambridge University Press, 2005, pp. 518-547.
- Leighton, T. G., Heald, G. J., Griffiths, H., Griffiths, G. (editors), 2001. *Acoustical Oceanography, Proceedings of the Institute of Acoustics* Vol. 23 Part 2, 2001.
- Leighton, T.G., Meers, S.D., White, P.R., 2004. Propagation through nonlinear time-dependent bubble clouds and the estimation of bubble populations from measured acoustic characteristics, *Proc. R. Soc. Lond. A*, **460**, 2521-2550.
- Leighton, T. G., Finfer, D. C., White, P. R., 2005(a) Bubble acoustics: What can we learn from cetaceans about contrast enhancement? *Proc. 2005 IEEE International Ultrasonics Symposium* (Rotterdam, 2005) pp. 964-973.
- Leighton, T. G., White, P. R., Finfer, D. C., 2005(b). The Sounds of Seas in Space. *Proceedings of the International Conference on Underwater Acoustic Measurements, Technologies and Results*, (J.S. Papadakis and L. Bjorno, eds.), 833-840.
- Leighton, T. G., White, P. R., Finfer, D. C., Grover, E. J. 2006. The sounds of seas in space: the 'waterfalls' of Titan and the ice seas of Europa, *Proceedings of the Institute of Acoustics*, 28(1), 2006, 75-97.
- Leighton, T. G., Finfer, D. C., White, P. R., 2007. Sound speed in the ocean of a small planet. ISVR Technical Report (in press).
- Mark, G., Tauber, A., Laupert, R., Schuchmann, H.P., Schulz, D., Mues, A., von Sonntag, C., 1998. OH-radical formation by ultrasound in aqueous solution. *Ultrasonics Sonochemistry*, 5, 41-52.
- Mason, T. J., Lorimer, J. P., Bates D. M., 1992. Quantifying sonochemistry : casting some light on a 'black art', *Ultrasonics* **30**, 40-42.
- Medwin, H., (editor), 2005. *Acoustical Oceanography: Sound in the Sea*, H. Medwin, Ed. Cambridge University Press.
- Melosh, H. J., Ekholm, A. G., Showman, A.P., Lorenz, R.D. 2004. The temperature of Europa's subsurface water ocean, *Icarus* **168**, 498-502.
- Merlino, R.L., 1997. Current-Driven Dust Ion Acoustic Instability in a Collisional Dusty Plasma, *IEEE Transactions on Plasma Science*, 25, 60-65.
- Munk, W. H., O'Reilly, W. C., Reid, J. L., 1988. Australia-Bermuda sound transmission experiment (1960) revisited. *J. Phys. Oceanogr.* **18**, 1876-1898.

- Nimmo, F., Schenk, P., 2006. Normal faulting on Europa: Implications for ice shell properties, *J. Struct. Geol.*, **28**, 2194–2203.
- Noyes, R.W., Jha, S., Korzennik, S.G., Krockenberger, M., Nisenson, P., Brown, T.M., 1997. A planet orbiting the star ρ Coronae Borealis, *The Astrophysical Journal*, **483**, L111–L114.
- Panning, M., Lekic, V., Manga, M., Cammarano, F., Romanowicz, B., 2006. Long-period seismology on Europa: 2. Predicted seismic response, *J. Geophysical Research*, **111**, E12009.
- Pappalardo, R. T., Head, J. W., Greeley, R., Sullivan, R. J., Pilcher, C., Schubert, G., Moore, W. B., Carr, M. H., Moore, J. M., Belton, M. J. S., Goldsby, D. L., 1998. Geological evidence for solid-state convection in Europa's ice shell, *Nature*, **391**, 365-368.
- Pieper, J. B., Goree, J., 1996. Dispersion of Plasma Dust Acoustic Waves in the Strong-Coupling Regime, *Physical Review Letters*, **77**, 3137-3140
- Rammacher, W., Ulmschneider, P., 1992. Acoustic waves in the solar atmosphere. IX- Three minute pulsations driven by shock overtaking. *Astron. and Astrophys.* **253**, 586-600.
- Rosenberg, M., Kalman, G. 1997. Dust acoustic waves in strongly coupled dusty plasmas, *Physical Review E*, **56**, 7166-7173.
- Sato, M., Itoh, H., Fujii, T., 2000. Frequency dependence of H₂O₂ generation from distilled water. *Ultrasonics*, **38**, 312-315.
- Schenk, P. M., McKinnon, W. B., 1989. Fault offsets and lateral crustal movement on Europa: Evidence for a mobile ice shell, *Icarus*, **79**, 75– 100.
- Shukla, P. K., 2000. Dust acoustic wave in a thermal dusty plasma, *Physical Review E*, **61**, 7249-7251.
- Sotin, C., 2007. Titan's lost seas found. *Nature*, **445**(7123), 29-30.
- Stofan, E. R., Elachi, C., Lunine, J. I., Lorenz, R. D., Stiles, B., Mitchell, K. L., Ostro, S., Soderblom, L., Wood, C., Zebker, H., Wall, S., Janssen, M., Kirk, R., Lopes, R., Paganelli, F., Radebaugh, J., Wye, L., Anderson, Y., Allison, M., Boehmer, R., Callahan, P., Encrenaz, P., Flamini, E., Francescetti, G., Gim, Y., Hamilton, G., Hensley, S., Johnson, W. T. K., Kelleher, K., Muhleman, D., Paillou, P., Picardi, G., Posa, F., Roth, L., Seu, R., Shaffer, S., Vetrella, S., West, R., 2007. The lakes of Titan. *Nature*, **445**, 61-64.
- The Planetary Society, 2007 (www.planetary.org/explore/topics/saturn/titan_sounds.html)
- Tokano, T., McKay, C. P., Neubauer, F. M., Atreya, S. K., Ferri, F., Fulchignoni, M., Niemann, H. B., 2006. Methane drizzle on Titan, *Nature*, **442**, 432-435.
- Verheest, F., 1993. Are weak dust-acoustic double layers adequately described by modified Korteweg-de Vries equations? *Physica Scripta*, **47**, 274-277.

- Zahnle, K., Dones, L., Levison, H. F., 1998. Cratering rates on the Galilean satellites. *Icarus* **136**, 202–222.
- Zarnecki, J. C., Leese, M. R., Hathi, B., Ball, A. J., Hagermann, A., Towner, M. C., Lorenz, R. D., McDonnell, J. A. M., Green, S. F., Patel, M. R., Ringrose, T. J., Rosenberg, P. D., Atkinson, K. R., Paton, M. D., Banaszekiewicz, M., Clark, B. C., Ferri, F., Fulchignoni, M., Ghafoor, N. A. L., Kargl, G., Svedhem, H., Delderfield, J., Grande, M., Parker, D. J., Challenor, P. G., Geake, J. E., 2005, A soft solid surface on Titan as revealed by the Huygens Surface Science Package, *Nature* **438**, 792-795.